

Number 544



**UNIVERSITY OF
CAMBRIDGE**

Computer Laboratory

On the support of recursive subdivision

I.P. Ivriissimtzis, M.A. Sabin, N.A. Dodgson

September 2002

An updated, improved version of this report has been published in ACM Trans. Graphics 23(4):1043–1060, October 2004
[doi:10.1145/1027411.1027417]

15 JJ Thomson Avenue
Cambridge CB3 0FD
United Kingdom
phone +44 1223 763500
<http://www.cl.cam.ac.uk/>

© 2002 I.P. Ivriissimtzis, M.A. Sabin, N.A. Dodgson

Technical reports published by the University of Cambridge
Computer Laboratory are freely available via the Internet:

<http://www.cl.cam.ac.uk/TechReports/>

ISSN 1476-2986

On the support of recursive subdivision

I. P. Ivriissimtzi^{*}, M. A. Sabin[†], N. A. Dodgson[‡]

September 2002

Abstract

We study the support of subdivision schemes, that is, the area of the subdivision surface that will be affected by the displacement of a single control point. Our main results cover the regular case, where the mesh induces a regular Euclidean tessellation of the parameter space. If n is the ratio of similarity between the tessellation at step k and step $k - 1$ of the subdivision, we show that this number determines if the support is polygonal or fractal. In particular if $n = 2$, as it is in the most schemes, the support is a polygon whose vertices can be easily determined. If $n \neq 2$, as for example in the $\sqrt{3}$ -scheme, the support is usually fractal and on its boundary we can identify sets like the classic ternary Cantor set.

1 Introduction

Recursive subdivision has recently emerged as one of the main tools for fast and efficient generation of high quality surfaces from an initial set of point data [12]. These points are considered as the vertices of a mesh, that is, they are connected by edges. An edge represents a path from one point to the other on an underlying surface in which the mesh is embedded. These paths tessellate the underlying surface into simply connected facets, encoding topological information. Subdivision can be described as a sequence of steps, each of which is a refinement operation. That is, in each step we add some new points, possibly dropping some of the existing ones, and connect them with edges, also possibly dropping some of the existing ones. This way we get a refined new mesh, and continuing the procedure, in the limit, we get a surface.

In this paper we deal with the support of recursive subdivision. That is, we are not studying the exact values of a subdivision surface but the set of non-zero values of the basis functions or, equivalently, the area of the surface that is affected by the change in position of a single vertex of the initial mesh. Such questions play an important rôle in both the application and the theoretical analysis of subdivision schemes.

Many of our methods are general and we will indicate how our results can be generalized to higher dimensions and irregular meshes, but first we study regular triangular and quadrilateral meshes.

1.1 Motivation

Our interest in this area was stimulated by preliminary analysis which indicated that Kobbelt's $\sqrt{3}$ scheme [8] had fractal support. We investigated whether this was true (it is), why it happens, and then generalized to consider all possible subdivision schemes. This paper presents our results.

The support of a scheme on the regular grid (either triangular or quadrilateral) is important for three principal reasons:

^{*}Max-Planck-Institut für Informatik (ivrissim@mpi-sb.mpg.de)

[†]Numerical Geometry Ltd (malcolm@geometry.demon.co.uk)

[‡]University of Cambridge Computer Laboratory (nad@cl.cam.ac.uk)

1. It shows the region in which the limit surface will change when a single control point is moved. The larger the support, the wider the influence of each control point. In general, schemes with compact support are preferred.
2. Its shape indicates the directions in which the scheme may have no lateral artifacts. For a direction to be free of lateral artifacts it is a necessary condition that there are two opposite edges to the support parallel to the direction in question.
3. If the scheme has fractal support than the basis function cannot consist of a finite number of polynomial pieces. We conjecture that this implies that there are no polynomial pieces in the limit surface except in special case configurations; one such case being where the surface is locally planar.

1.2 Overview

In Section 2 we give necessary basic definitions, introduce some special terminology, and give a brief introduction to the Cantor sets, which play an important rôle in the study of the support.

In Section 3 we describe the method we use to calculate the support. We see the parameter space as a vector space, and the main result is that the points of the support can be written as well-defined infinite sums of elements of this vector space.

In Section 4 we use this method to prove propositions on the support of univariate schemes.

In Section 5 we use the univariate results to study the boundary of the convex hull of the support of bivariate schemes. This convex hull gives an outer bound of the support, and then we identify polygonal areas inside the support, whose union gives an inner bound.

In Section 6 we deal in more detail with two examples illustrating the above.

In the final sections we briefly describe possible generalizations of the method, discuss some implications of our results into the artifact analysis of subdivision schemes, and conclude with a brief summary.

2 Terminology and background theory

In this paper we use certain terms with specific meanings:

A *polyhedron* is a set of vertices, edges and faces. The vertices have position, and the edges and faces are defined solely by the vertices which they join. It is not quite a geometric polyhedron, where the faces would need to be planar, nor is it a topological one, where there would be no geometry at all.

For most of this paper we concern ourselves with the regular situation where every vertex has the same number of incident edges and faces. We do not concern ourselves here with edge conditions because the issue we address is a local one.

In addition to considering the regular case, the analysis needs to be extended to polyhedra which have regions which are not topologically equivalent to a regular tessellation. A polyhedron of general genus must have *extraordinary points*, vertices or faces with other than the regular number of neighbors. This irregular case is dealt with in Section 7.

Subdivision is the process whereby an initial polyhedron is treated as the data from which a polyhedron with more vertices, edges and faces is set up. The new vertices are affine combinations of old ones, with coefficients defined by the particular *scheme*. The new connectivity is also defined by the scheme.

The coefficients of a scheme can be documented in either of two ways:

- The *mask* is the set of coefficients by which a given old vertex influences the new ones at each refinement. It is presented as a diagram showing the non-zero coefficients laid out in the same arrangement as the new vertices relative to the old one. An example is shown in Figure 1(a). In the regular grid case, both old and new vertices are laid out in a regular array, either quadrilateral or triangular, in what we may think of as a parametric space. This provides the domain for the mask diagram and also for other objects defined in this section.

$$\begin{array}{ccc}
 & & \begin{array}{cc} \text{vertex} & \text{horizontal edge} \end{array} \\
 & & \frac{1}{64} \begin{bmatrix} 1 & 6 & 1 \\ 6 & 36 & 6 \\ 1 & 6 & 1 \end{bmatrix} \quad \frac{1}{64} \begin{bmatrix} 4 & 4 \\ 24 & 24 \\ 4 & 4 \end{bmatrix} \\
 \frac{1}{64} \begin{bmatrix} 1 & 4 & 6 & 4 & 1 \\ 4 & 16 & 24 & 16 & 4 \\ 6 & 24 & 36 & 24 & 6 \\ 4 & 16 & 24 & 16 & 4 \\ 1 & 4 & 6 & 4 & 1 \end{bmatrix} & & \begin{array}{cc} \text{vertical edge} & \text{face} \end{array} \\
 & & \frac{1}{64} \begin{bmatrix} 4 & 24 & 4 \\ 4 & 24 & 4 \end{bmatrix} \quad \frac{1}{64} \begin{bmatrix} 16 & 16 \\ 16 & 16 \end{bmatrix} \\
 \text{(a)} & & \text{(b)}
 \end{array}$$

Figure 1: (a) the *mask* and (b) the *stencils* of the Catmull-Clark subdivision scheme which is used on the quadrilateral grid [2].

- A *stencil* is the set of coefficients by which a given new vertex is influenced by the old ones¹. It is presented as a diagram showing the non-zero coefficients laid out in the same arrangement as the old vertices relative to the new one. Examples are shown in Figure 1(b).

There is one stencil for each distinct relationship between the new vertices and the old, whereas there is only one mask. Masks and stencils form the columns and rows of the subdivision matrix by which the vector of old vertices is multiplied to give the new ones. This is clear in the univariate case but still true in the multivariate case. The mask and the stencils therefore contain exactly the same information. This relationship is illustrated in the example in Figure 1, where it can be easily seen that each stencil can be extracted from the mask by starting at one of the 2×2 lower left values and then taking every second element both horizontally and vertically².

The *arity* is the ratio of similarity between the edge of the initial regular mesh and the edge of the mesh after one subdivision step. The schemes with arity 2 are called binary, the schemes with arity 3 are called ternary, etc. The arity is well-defined because, owing to the symmetry assumptions underlying a subdivision scheme, the subdivision of a regular mesh is also regular. In fact, this property was used in [1] and [6] for a classification of all the subdivision schemes. The arity, usually, is either an integer or the square root of an integer. Here we consider schemes with integer arity and study the square root schemes by taking double steps. Nevertheless, most of the propositions and their proofs can handle any arity.

The *footprint* is the set of points with non-zero coefficients in the mask. Because it is laid out in the domain in the same way as the mask, we can refer to the convex hull of the footprint without confusion. It is denoted by \mathbf{F} .

The *scaled footprint* is the footprint scaled up by $\frac{n}{n-1}$, where n is the arity. It will be denoted by \mathbf{F}' .

The *basis function* is the map from positions in the domain to the limit surface of the refinement corresponding to a single old vertex having a unit value and all the others zero. It may also be thought of as the limit of a sequence of masks obtained by repeatedly convolving the previous member of the sequence with the mask.

The *support* is the closure³ of the points whose values are non-zero in the basis function. It may also be thought of as the closure of the sequence of footprints of the masks which converge to the basis function. It will be denoted by \mathbf{S} .

The *ternary Cantor set* was introduced in the 19th century as an example of an infinite, uncountable set with measure zero. An introduction to it can be found in [7]. The most well-known construction of the ternary Cantor set is by repeated removal of intervals from the interval (0,1)

¹Note that some authors use the term ‘masks’ to refer to what we here call ‘stencils’.

²Technically, one should reflect the mask in the origin before extracting the stencils in this way. In this case, the reflection produces the same mask.

³Note that the support, defined as the inverse image of $\mathbb{R}^n \setminus 0$ under a continuous map, must be open. The closure is taken so that the zero contours of the basis functions of interpolating schemes, where the basis function typically has both positive and negative regions, remain within the support.

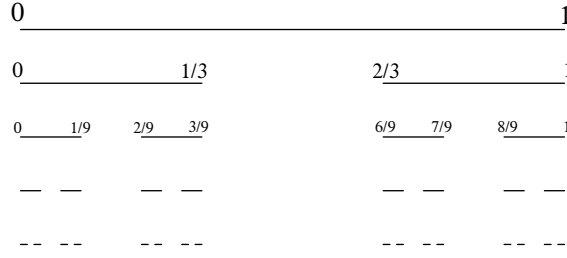


Figure 2: The first four steps in the construction of the ternary Cantor set with repeated removal of middle third intervals.

of real numbers. In the first step we remove the middle third interval $(\frac{1}{3}, \frac{2}{3})$, in the second step we remove the intervals $(\frac{1}{9}, \frac{2}{9})$ and $(\frac{7}{9}, \frac{8}{9})$, and, continuing this way, at each step we remove the middle third interval from each one of the existing intervals. The limit of this process is the ternary Cantor set. Figure 2 shows four consecutive steps in the construction of the ternary Cantor set by removal of intervals. Some alternative descriptions of the Cantor set are given in the Appendix at the end of the paper.

The *Cantor like sets* are generalizations of the ternary Cantor set. In each case some intervals are removed from the interval $(0,1)$ and we get a not connected set A . Then, in a self similar fashion, this process is repeated, with intervals removed from every component of A , or equivalently, by substituting every component of A with a scaled image of A .

3 Description of the method

In our study of the support, starting from the initial control mesh of the basis function, we create a sequence

$$S_1, S_2, S_3, \dots \quad (1)$$

of subsets of the domain, each one corresponding to one step of the subdivision process. Examples are shown in Figures 3 and 4.

The first set S_1 consists of the points of the domain having non-zero z -coordinate after one subdivision step. That is, S_1 is the footprint of the scheme

$$S_1 = \{P_0, P_1, P_2 \dots P_k\} \quad (2)$$

where P_i is the i^{th} point in the mask. Having fixed the origin O , the points of the domain \mathbb{R}^2 are in an 1-1 correspondence with the displacements from the origin. Although the analysis works for any choice of origin, the assumption that the origin is at the centre of symmetry of the mask is a convenient one. In particular, the point P_i corresponds to the displacement \vec{OP}_i and under this correspondence the domain \mathbb{R}^2 inherits the vector space structure of the displacements, allowing us to define an addition between points as well as a multiplication of the points by numbers.

If n is the arity of the scheme, and because of the self-similarity of the subdivision process, the points with non-zero z -coordinate after the second step are given by

$$S_2 = \{P_i + \frac{1}{n}P_j \mid i, j = 0, \dots k\} \quad (3)$$

The set S_2 can be thought of as being obtained from S_1 by substituting each of the points of S_1 with an image of S_1 scaled down by a factor of n . Continuing recursively we define the set

$$S_m = \left\{ P + \frac{1}{n^{m-1}}P_i \mid P \in S_{m-1}, i = 0, 1, \dots k \right\} \quad (4)$$

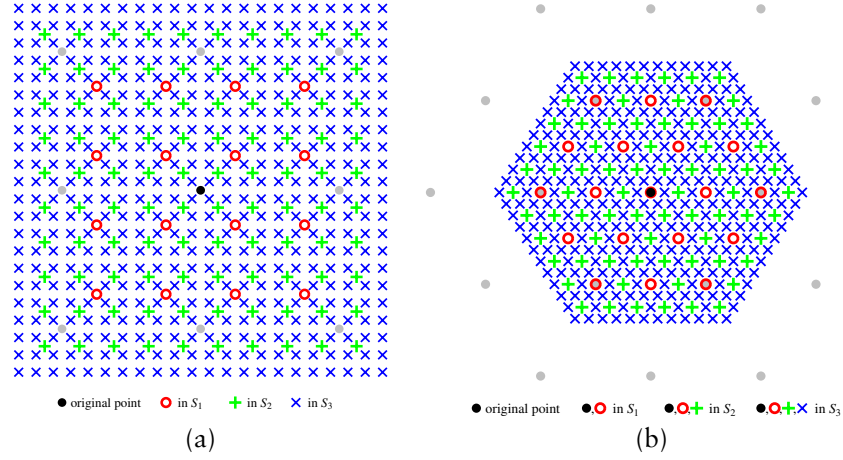


Figure 3: The first four point sets for (a) Doo-Sabin [5] and (b) Loop [9] schemes. The black dot in the center represents the original vertex under consideration. The pale grey dots represent other vertices of the original grid, thereby showing the relationship between the original grid and the point sets. Note that, in the Loop scheme, S_1 contains the vertices in the 1-ring of the original vertex. Both schemes have polygonal support ((a) square, (b) hexagonal) in the limit.

obtained from S_{m-1} by substituting each of its points with an image of S_1 scaled down by a factor of n^{m-1} . S_m can also be written

$$S_m = \left\{ P_{i_1} + \frac{1}{n} P_{i_2} + \dots + \frac{1}{n^{m-1}} P_{i_m} \mid i_1, i_2, \dots, i_m = 0, 1, \dots, k \right\} \quad (5)$$

Figure 3 illustrates the point sets S_1 , S_2 , and S_3 for the Doo-Sabin quadrilateral [5] and Loop triangular [9] schemes respectively.

To find the total support we have to define a limit for the sequence of sets (1) and then take the closure, that is

$$\mathbf{S} = \overline{\lim_{m \rightarrow \infty} S_m} \quad (6)$$

Figure 4 shows two interesting cases with S_4 offering a good approximation to \mathbf{S} . Notice that the topological operator closure, which adds to a set its points of accumulation, has a double effect. Firstly, by adding the points of accumulation in general, we make sure that we get a smooth surface and not a dense cloud of points. Indeed, after taking the closure we do not even need to consider the limit of a sequence of progressively refined meshes, as it is usually the case in the study of subdivision. Secondly, by adding the points of accumulation with zero z -coordinate in particular, we include the zero contours of oscillatory schemes with negative coefficients, complying this way with the definition of the support we gave in Section 2.

An arithmetic definition of the limit in Eq. (6), analogous to Eq. (5), is given by the infinite sums

$$\mathbf{S} = \left\{ \sum_{m=1}^{\infty} \frac{1}{n^{m-1}} P_{i_m} \mid i_m = 0, 1, \dots, k \right\} \quad (7)$$

describing the support as the set of all possible infinite affine combinations of points of the footprint, with coefficients following a geometric progression with ratio $\frac{1}{n}$.

Any of the infinite sums in Eq. (7) is the limit of its initial partial finite sums, that is, the limit of a sequence of points

$$\mathbf{p}_1, \mathbf{p}_2, \dots \quad \text{with} \quad \mathbf{p}_m \in S_m, \quad m = 1, 2, \dots \quad (8)$$

showing the equivalence of Eq. (6) and Eq. (7). Notice that for $n > 1$ the partial initial sums in Eq. (7) converge, and thus the infinite sum is well-defined. Also notice that the set defined in Eq. (7) is closed and we do not need to use the topological operator closure.

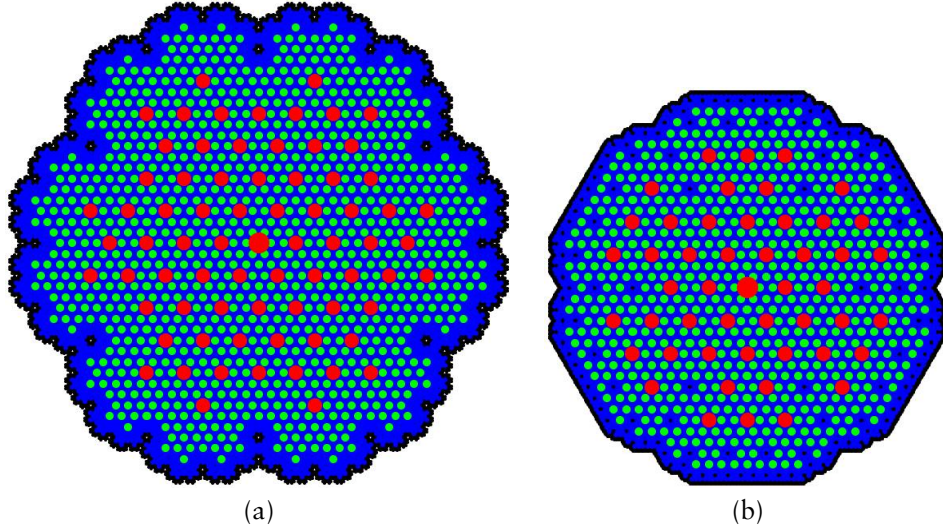


Figure 4: The initial control net of the basis function has a unique point with non-zero z -coordinate. The non-zero points after the first iteration are shown in red. The non zero points after the second step are shown in green. These green points are obtained by substituting every red point with a scaled image of the set of red points. Continuing this recursive process we find the non-zero points after three steps (blue) and four steps (black). The limit of this process is the *support*. (a) The $\sqrt{3}$ -scheme with double steps. (b) A ternary butterfly scheme.

Eq. (7) can also be written in terms of the points of the scaled footprint in the scaled form

$$\mathbf{S} = \left\{ \sum_{m=1}^{\infty} \frac{n-1}{n^m} P'_{i_m} \mid i_m = 0, 1, \dots, k \right\} \quad (9)$$

with $P'_i \in \mathbf{F}'$, that is,

$$P'_i = \frac{n}{n-1} P_i, \quad i = 0, 1, \dots, k \quad (10)$$

The coefficients in Eq. (9) sum to 1 and, thus, the points of the support are written as convex combinations of the points of the scaled footprint. By Eq. (9) the convex hull of the scaled footprint contains the support \mathbf{S} , and we use this convex hull as an outer bound for \mathbf{S} . In fact, the converse inclusion also holds and thus the convex hull of the scaled footprint is the convex hull of the support. The latter is a direct corollary of Eq. (9) for

$$i_1 = i_2 = \dots = i_m = \dots \quad (11)$$

Thus Eq. (9) is the basic equation with which we work, describing the support in terms of the arity and the scaled footprint only. The rest of the paper is devoted to the study of this equation for different configurations of the scaled footprint and different values of n .

4 The univariate case

Although the support of all the known univariate schemes can be calculated easily, we will give some formal proofs for univariate schemes, because we will use them in the boundary analysis of the bivariate schemes, and also as motivation for the bivariate case, where the techniques are similar.

In the univariate case the domain is \mathbb{R} rather than \mathbb{R}^2 . It is thus an ordered set. We first assume that the footprint consists of $k+1$ equispaced points. We have:

Proposition 4.1 *If the footprint of a univariate scheme consists of $k+1$ equispaced points P_0, P_1, \dots, P_k , then we have*

(i) *if $k < n - 1$ then \mathbf{S} is a Cantor like fractal set.*

(ii) *if $k \geq n - 1$ then \mathbf{S} is the interval defined as the convex hull of the scaled footprint, that is,*

$$\mathbf{S} = \left[\frac{n}{n-1}P_0, \frac{n}{n-1}P_k \right]. \quad (12)$$

Proof: As the scaled footprint is the scaled image of the footprint, its points are also equispaced, thus, we have

$$P'_i = \frac{k-i}{k}P'_0 + \frac{i}{k}P'_k, \quad i = 0, 1, \dots, k. \quad (13)$$

Then, Eq. (9) becomes

$$\mathbf{S} = \left\{ \sum_{m=1}^{\infty} \frac{(k-i_m)(n-1)}{kn^m} P_0 + \sum_{m=1}^{\infty} \frac{i_m(n-1)}{kn^m} P'_k \mid i_m = 0, 1, \dots, k \right\} \quad (14)$$

and the support is the point set

$$(1-\lambda)P_0 + \lambda P_k \quad (15)$$

with

$$\lambda \in A = \left\{ \sum_{m=1}^{\infty} \frac{i_m(n-1)}{kn^m} \mid i_m = 0, 1, \dots, k \right\} \quad (16)$$

The self-similarity of the subdivision process can be expressed numerically by writing the infinite sum in (16) as

$$\sum_{m=1}^{\infty} \frac{i_m(n-1)}{kn^m} = \frac{i_1(n-1)}{kn} + \sum_{m=2}^{\infty} \frac{i_m(n-1)}{kn^m} = \frac{i_1(n-1)}{kn} + \frac{1}{n} \sum_{m=1}^{\infty} \frac{i_{m+1}(n-1)}{kn^m} \quad (17)$$

or, in a set-theoretic notation

$$A = \bigcup_{i=0}^k \left(\frac{i(n-1)}{kn} + \frac{1}{n}A \right) \quad (18)$$

with each component of the union corresponding to a choice of a value for i_1 .

If $k < n - 1$ then the above is a Cantor like fractal set. Indeed, the convex hull of A is the interval $[0,1]$ and thus, the convex hull of each of the components of (18) is an interval of length $\frac{1}{n}$. Figure 5(a) shows the convex hulls of the components of (18). The union of these convex hulls gives an improved outer bound for A , which is a proper subset of the interval $[0,1]$. Continuing this way, choosing i_2, i_3, \dots and splitting each interval into $k + 1$ parts, in the limit we obtain a Cantor like set.

If $k = n - 1$ then the sets of (18) have convex hull of length $\frac{1}{n}$ and cover the interval $[0, 1]$ (Figure 5(b)). In fact, in this case we can observe that Eq. (16) gives the expression of each $\lambda \in [0, 1]$ in the n -adic system, and so $A = [0, 1]$.

Intuitively, it is obvious that $A = [0, 1]$ also holds for $k > n - 1$. For a formal proof we notice that in this case the convex hulls of the sets of (18) again cover the interval $[0,1]$. Their intersection is now an interval, while in the case $k = n - 1$ it is just a point (Figure 5(c)). In the next step each of these intervals is again covered by a set of $k + 1$ intervals, similar to A with ratio $\frac{1}{n^2}$, and so on. For each point of $[0,1]$ we can find a nested sequence of intervals, one interval from each subdivision step, converging to that point. From this sequence we can obtain the coefficients i_m giving this point in the form of Eq. (16). \square

The next proposition is a generalization of the previous one for footprints with unequally spaced points. We will not give an exact description of the resulting sets but we will find when the support is the interval defined as the convex hull of the scaled footprint and when it is a Cantor like set.

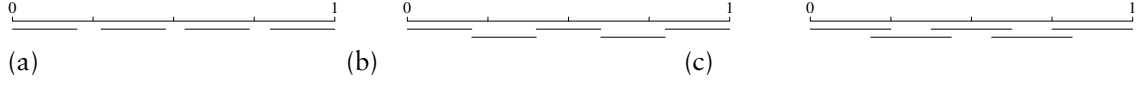


Figure 5: (a) If $k < n - 1$ the convex hulls of the components of (18) do not cover the interval $(0, 1)$. (b) If $k = n - 1$ the convex hulls do cover $(0, 1)$ and intersect between them on points. (c) If $k > n - 1$ they cover $(0, 1)$ and intersect on intervals.

Proposition 4.2 *The support is the whole interval $[P'_0, P'_k]$ if and only if*

$$|P_i - P_{i-1}| \leq \frac{|P_k - P_0|}{n-1}, \quad i = 1, \dots, k \quad (19)$$

Proof: We will only outline the proof as the ideas are essentially the same as Proposition 4.1. By evaluating the first coefficient in Eq. (9) we create a split of \mathbf{S} into k subsets similar to it. Their convex hulls are intervals of length $\frac{|P_k - P_0|}{n}$ and they cover $[P_0, P_k]$ exactly when (19) holds. If this is the case, then by consecutively evaluating all the coefficients of (9), and using the self-similarity, we produce a sequence of coverings of $[0, 1]$. Any point of $[0, 1]$ can be lifted in a sequence of intervals, one interval for each covering, and this sequence gives the coefficients of the point written in the form (9).

With similar arguments we can see that \mathbf{S} is a Cantor like set when (19) does not hold. \square

4.1 Example

In [3] a general (n, k) interpolatory univariate scheme was described as the process of inserting between any two consecutive existing points, $n - 1$ equally spaced new ones, defined as affine combinations of the $2k$ nearest already existing points. In that case we have

$$S_1 = \left\{ -k + \frac{1}{n}, -k + \frac{2}{n}, \dots, k - \frac{1}{n} \right\} \quad (20)$$

and by Proposition 4.1 the support of that scheme is the interval

$$\left[\frac{n}{n-1} \left(-k + \frac{1}{n} \right), \frac{n}{n-1} \left(k - \frac{1}{n} \right) \right] \quad (21)$$

5 The bivariate case

5.1 The boundary of the convex hull of the support

Going to the bivariate case we start with propositions about the boundary of the convex hull of the support. Then we study polygonal areas inside the support, trying to find criteria to determine when they are subsets of the support.

As we have already seen the convex hull of \mathbf{S} is the convex hull of the scaled footprint \mathbf{F}' . Its boundary is a polygon and we can cyclically enumerate the vertices of the scaled footprint that lie on this boundary (Figure 6). Notice that the convex hull of the points lying on the boundary and the convex hull of the whole \mathbf{F}' are the same. In fact, the vertices of that polygon would suffice to describe the convex hull.

The first question is: when is an edge of the boundary part of the support? The main observation is that, while the points of \mathbf{S} in general are convex combinations of the points of \mathbf{F}' , the points of \mathbf{S} lying on an edge of the convex hull in particular are convex combinations of the points of \mathbf{F}' lying on that edge. That means that if $Q_0 Q_l$ is an edge of the convex hull, containing the points Q_0, Q_1, \dots, Q_l of \mathbf{F}' , then Eq. (9) becomes

$$\mathbf{S}_e = \left\{ \sum_{m=1}^{\infty} \frac{n-1}{n^m} Q_{i_m} \mid i_m = 0, 1, \dots, l \right\} \quad (22)$$

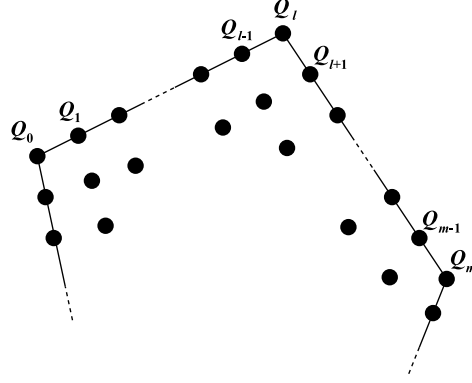


Figure 6: An enumeration of the points which lie on the convex hull of the scaled footprint.

where S_e is the intersection of S with Q_0Q_l . The problem is thus reduced to the univariate case. Hence, from Proposition 4.1 we get

Proposition 5.1 *If the points Q_0, Q_1, \dots, Q_l are equispaced, then the edge Q_0Q_l is contained in S if and only if $l \geq n - 1$. Otherwise, the intersection of Q_0Q_l and S is a Cantor like set.*

Although the points Q_0, Q_1, \dots, Q_l of Proposition 5.1 are aligned on a line of a regular mesh, they need not be equally spaced, as they can form a proper subset of the intersection of the interval Q_0Q_l with the vertices of the regular mesh. For that case, from Proposition 4.2 we have the more general

Proposition 5.2 *The whole edge Q_0Q_l is contained in S if and only if all pairs of consecutive points Q_{i-1}, Q_i on the edge obey the inequality*

$$|Q_{i-1}Q_i| \leq \frac{|Q_0Q_l|}{n-1}, \quad i = 1, \dots, l \quad (23)$$

Otherwise the intersection of Q_0Q_l and S is a Cantor like, not connected set.

As an immediate corollary of the above propositions we have this special case which is very often met in practice

Corollary 5.1 *Let Q_0Q_1 be an edge of the scaled footprint, that is, there are no other points Q_i in the interior of that edge. If the scheme is binary then the edge Q_0Q_1 is in S . If $n > 2$ then the intersection of S with the edge Q_0Q_1 is a Cantor like set defined on the that edge.*

5.2 Polygonal subsets of the support

The propositions on the convex hull of S and its boundary give us an outer bound for the support, as well as an indication for the behavior of S near this outer bound. We next try to identify polygonal areas inside that convex hull that are subsets of S , finding this way an inner bound for S .

From Eq. (9) we notice that the support corresponding to a subset of F' is itself a subset of S . Thus, by finding subsets of F' with polygonal support we find polygonal areas of the total support. Then by taking the union of these polygonal areas we can find a polygonal inner bound for S .

We study three particular configurations of scaled footprints, thought of here as subsets of the original scaled footprint. Namely, the cases where the points of F' form a parallelogram, a hexagon, or an equilateral triangle. We find conditions under which the corresponding support is equal to the convex hull of F' .

The simplest case occurs when the scaled footprint has a tensor product structure, that is, when the points form a parallelogram. We have

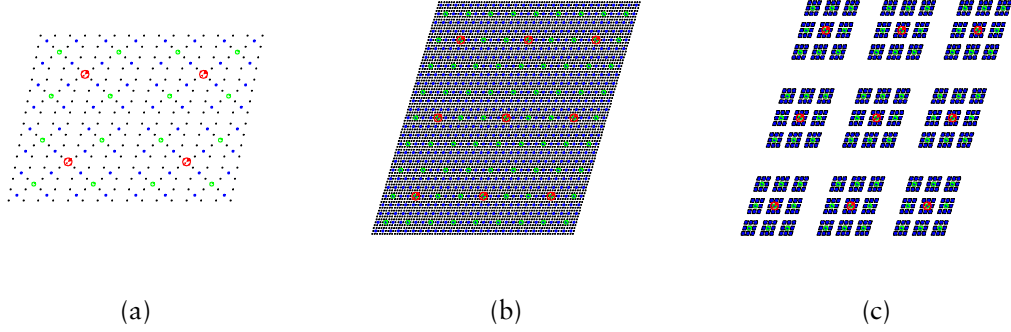


Figure 7: The support of a tensor product is the tensor product of the supports. (a) $i = j = 1$, $n = 2$. (b) $i = j = 2$, $n = 3$. (c) $i = j = 2$, $n = 4$. The first two examples have polygonal support while the third has fractal support.

Proposition 5.3 *Let \mathbf{F}' be the tensor product $A \times B$ of two sets of collinear points*

$$A = \{A_0, A_1, \dots, A_i\} \quad \text{and} \quad B = \{B_0, B_1, \dots, B_j\} \quad (24)$$

with $A_0 = B_0$ and $A_0\vec{A}_i, B_0\vec{B}_j$ linearly independent. Then \mathbf{S} is the tensor product of the supports of A and B .

Proof: Any point of \mathbf{F}' has the form

$$A_s + B_t, \quad s = 0, 1, \dots, i \quad t = 0, 1, \dots, j \quad (25)$$

while the points of \mathbf{S} have the form

$$P = \frac{n-1}{n} (A_{s_1} + B_{t_1} + \frac{1}{n}(A_{s_2} + B_{t_2}) + \frac{1}{n^2}(A_{s_3} + B_{t_3}) + \dots) \quad (26)$$

From (26) we can find the projections

$$P_A = \frac{n-1}{n} (A_{s_1} + \frac{1}{n}A_{s_2} + \frac{1}{n^2}A_{s_3} + \dots) \quad (27)$$

$$P_B = \frac{n-1}{n} (B_{t_1} + \frac{1}{n}B_{t_2} + \frac{1}{n^2}B_{t_3} + \dots) \quad (28)$$

that belong in the supports of A and B corresponding. Conversely, starting with the points P_A, P_B on the supports of A, B , we find the point $P = P_A + P_B$ in \mathbf{S} , by component-wise summation. \square

Figure 7 shows some examples for the above proposition.

The hexagonal case can be readily reduced to the tensor product case.

Proposition 5.4 *Let the points of \mathbf{F}' form a regular hexagonal mesh with $m + 1$ vertices on each edge. The convex hull of \mathbf{F}' is a subset of \mathbf{S} if and only if $m \geq n - 1$.*

Proof: First let $m \geq n - 1$. We separate the hexagonal mesh \mathbf{F}' into three parallelograms as shown in Figure 8(a) for $m = 2$. By Propositions 4.1 and 5.3 each of them is a subset of \mathbf{S} and so the whole hexagon is a subset of \mathbf{S} . If $m < n - 1$ then by Proposition 4.1 the edges of the hexagon are not subsets of \mathbf{S} and so \mathbf{S} does not contain the whole hexagon. \square

Figure 8(b) shows an example with fractal support. Figure 8(c), one with polygonal support.

The triangular case is essentially different. We have

Proposition 5.5 *Let the points of \mathbf{F}' form a regular triangular mesh with $m + 1$ vertices on each edge. Then the support \mathbf{S} is equal to the convex hull of \mathbf{F}' if and only if $m \geq 2n - 2$.*

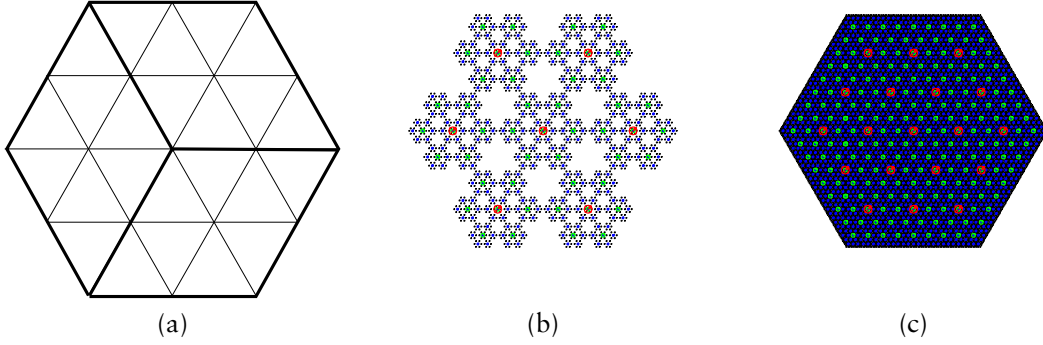


Figure 8: (a) We divide the hexagon into 3 parallelograms. (b) The support for $m = 1$, $n = 3$. (c) The support for $m = 2$, $n = 3$.

Proof: First let $m \geq 2n - 2$. We can cover \mathbf{F}' , with parallelograms having $\lfloor \frac{m}{2} \rfloor + 1$ and $\lceil \frac{m}{2} \rceil + 1$ vertices on its edges (Figure 9(a)). Then $m \geq 2n - 2$ gives $\lfloor \frac{m}{2} \rfloor + 1 \geq n - 1$, and by Propositions 4.1 and 5.3 each of these parallelograms is a subset of \mathbf{S} and so their union is also a subset of \mathbf{S} .

Suppose now that $m = 2n - 3$. Each point of the scaled footprint \mathbf{F}' , and indeed each point of the support \mathbf{S} , can be written in a unique way in the form of the barycentric coordinates defined by the vertices of the triangle:

$$\alpha A + \beta B + \gamma C \quad \text{with} \quad 0 \leq \alpha, \beta, \gamma \quad \text{and} \quad \alpha + \beta + \gamma = 1 \quad (29)$$

The equation $\beta = \gamma$ gives the segment with end points A and A' where A' is the midpoint of BC . We will show that Eq. (9) can not generate the subinterval of AA' defined by

$$\frac{1}{2n} \leq \beta = \gamma \leq \frac{n-1}{n} \frac{1}{2n-3} \quad (30)$$

See Figure 9(b).

Indeed, first let $P_{i_1} \neq A$. Then, for all the other points of \mathbf{F}' written in the form (29), we have

$$\frac{1}{2n-3} \leq \beta \quad \text{or} \quad \frac{1}{2n-3} \leq \gamma \quad (31)$$

and for the point corresponding to the first component of the infinite sum in (9) we have

$$\frac{n-1}{n} \frac{1}{2n-3} \leq \beta \quad \text{or} \quad \frac{n-1}{n} \frac{1}{2n-3} \leq \gamma \quad (32)$$

Eq. (32) also holds for the total sum in (9), showing that all the points of \mathbf{S} given by (9) are outside the interval defined by (30).

On the other hand, if $P_{i_1} = A$ then (9) gives

$$\beta + \gamma \leq \sum_{m=2}^{\infty} \frac{n-1}{n^m} = \frac{1}{n} \quad (33)$$

giving,

$$\beta \leq \frac{1}{2n} \quad \text{or} \quad \gamma \leq \frac{1}{2n} \quad (34)$$

showing that it is again outside the interval in (30). \square

Figure 10 shows two examples for $n = 2$ and one for $n = 3$, all of which have fractal support.

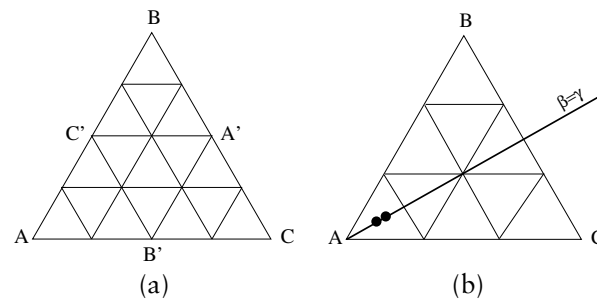


Figure 9: (a) $m = 4$, $n = 3$, we cover the lattice triangle with three parallelograms $AC'A'B'$, $BA'B'C'$, $CB'C'A'$. (b) The bold line satisfies the equation $\beta = \gamma$. The two thick points on it define an interval which is not part of the support.

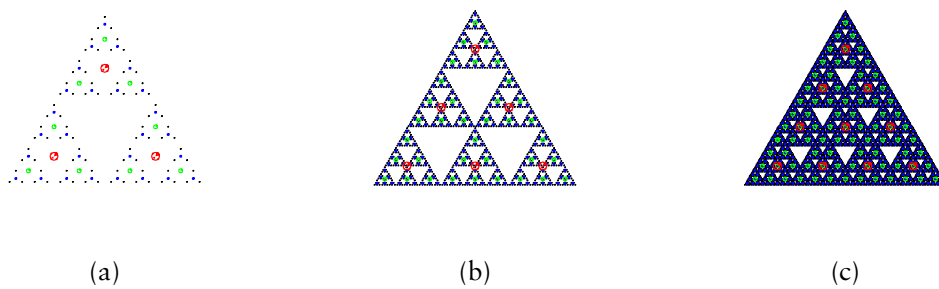


Figure 10: The support when F' is a lattice triangle. (a) $m = 1$, $n = 2$. (b) $m = 2$, $n = 3$. (c) $m = 3$, $n = 3$. Notice that the triangular case is the only one where arity $n = 2$ may produce a fractal.

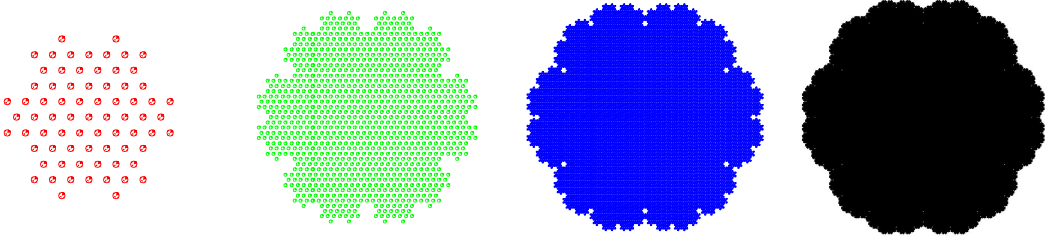


Figure 11: The red point set shows the footprint S_1 of a double step of the $\sqrt{3}$ -scheme. The other point sets are S_2 , S_3 and S_4 , respectively.

6 Examples

Figures 7, 8 and 10 show simple examples. Figure 3 shows two well-known binary schemes; it is easy to see that these two schemes have polygonal support. In this section we deal in detail with two particular examples of subdivision schemes which have more interesting behaviour. Both have arity $n = 3$, as we saw that it is trivial to find the support of binary schemes such as those shown in Figure 3.

6.1 The $\sqrt{3}$ scheme

The $\sqrt{3}$ scheme was recently proposed in [8]. In each step a new vertex is inserted at the barycenter of each triangle, and every old vertex is relaxed according to an affine combination of itself and its direct neighbors. After two iterations, and so for any even number of iterations, the scheme becomes a proper ternary scheme, that is $n = 3$. Here we study the support of this ternary scheme defined by double steps of the $\sqrt{3}$ scheme, which is, of course, the same as the support of the original $\sqrt{3}$ -scheme.

Figure 11 shows the sets S_1 , S_2 , S_3 and S_4 , that is the non-zero points of the basis function constructed after 1, 2, 3 and 4 steps, respectively. Figure 4(a) shows a superimposition of these sets.

In Figure 12(a) the red points represent the scaled footprint. The black area represents the part of the support constructed after four iterations, giving an indication of the shape of the total support. The blue polygon is the convex hull of the scaled footprint, and so the convex hull of the support, and it is a polygonal outer bound for the support. This polygon is a dodecagon, which is not regular as it has 6 shorter edges and 6 longer. There are no other vertices of the scaled footprint on these twelve edges, so by Proposition 5.2 their intersection with the support are the ternary Cantor sets defined on them.

The green dashed polygon is an inner bound that was constructed with the use of Proposition 5.3. It is worth noticing that it is by no means trivial to find the optimal inner bound which the use of Propositions 5.3, 5.4, 5.5 can give. In fact, it is a very interesting combinatorial problem. For example, each of the vertices of the boundary dodecagon belongs to a triangle of \mathbf{F}' with 7 vertices on each edge, which by Proposition 5.5 belongs to the support. These twelve triangles will give a good inner bound which nevertheless will not be optimal. For a better inner bound we consider the three parallelograms with 5 and 7 vertices on each edge shown in Figure 12(b). By Proposition 5.3 they belong to the support and give a better inner bound.

If we wanted to improve on this bound we could study the 9-ary scheme with step equal to four steps of the $\sqrt{3}$ -scheme. The footprint of this scheme is shown in Figure 11 (green points). Notice that now each edge of the boundary of the convex hull contains 4 points of the scaled footprint.

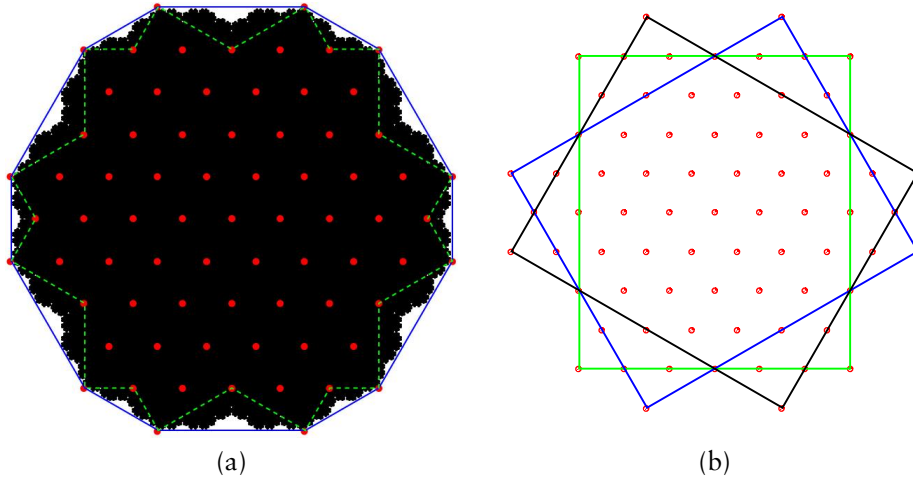


Figure 12: (a) The black area (S_4) is an approximation to S after four iterations. The red points are the scaled footprint F' . The blue line and the green dashed line give an outer and an inner polygonal bound for S . (b) We show three parallelograms that are subsets of the support. Their union gives the inner polygonal bound of S : the green dashed line in (a).

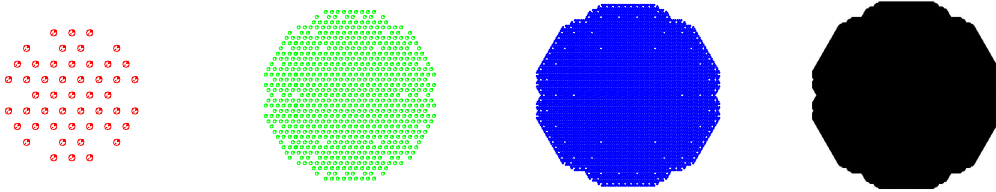


Figure 13: The red point set shows the footprint S_1 of a ternary butterfly scheme. The other point sets are S_2 , S_3 and S_4 , respectively.

6.2 A ternary butterfly scheme

The second example (Figures 13 and 4(b)) is a ternary version of the butterfly scheme, contrived to illustrate the possibility that fractal behaviour may occur on some edges of the support but not all (this is the scheme described in [4] with the parameter values $\nu = \epsilon = 0$). Here there are some negative coefficients, so some of the results hold under the assumption that the support also includes the zero contour lines.

The convex hull of the support S is again a dodecagon with 6 short edges and 6 long. By Proposition 4.1 the intersection of the short edges with S is a ternary Cantor set, while the long edges belong to S .

On the scaled footprint we can identify six parallelograms, shown in Figure 14(b), belonging to the support. Their union gives the optimal inner bound we can obtain with the use of the propositions we have proved. Notice that one type of parallelogram has non-equispaced points on one of its edges, therefore, in conjunction with Proposition 5.3 we have to use the more general Proposition 4.2.

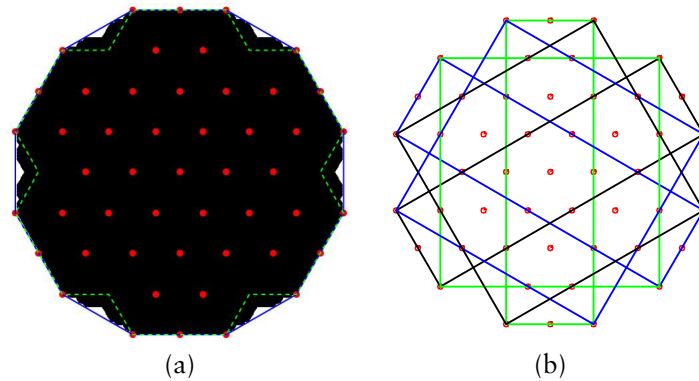


Figure 14: (a) The black area (S_4) is an approximation to S after four iterations. The red points are the scaled footprint F' . The blue line and the green dashed line give an outer and an inner polygonal bound for S . (b) We show six parallelograms that are subsets of the support. Their union gives the inner polygonal bound of S : the green dashed line in (a). Notice that there are two types of parallelograms. The more square of the parallelograms have non-equispaced points of F' on two edges.

7 Generalizations

In this section we consider first the important case of irregular connectivity in the polyhedron and then look at other generalizations of this work to the study of skew schemes and the study of higher dimensional schemes.

7.1 The irregular case

The above has considered only the case where the connectivity of the polyhedron is totally regular, forming either a quadrilateral or a triangular grid.

The main problem in the irregular case, where extraordinary points are present, is that we no longer have a well-defined domain. Nevertheless, we may make certain observations which we expect to give true conclusions.

We consider first the mask and support of an isolated extraordinary point. The configuration has n -fold symmetry around this point rather than the usual 4- or 6-fold. However, the pattern within each of the 4 or 6 sectors of the regular case now appears within each of the n sectors of the extraordinary point mask. The parts of the mask at the next subdivision level which influence the support are not interfered with by the extraordinary vertex itself, and so we assert that the nature (polygonal or fractal) of the support in each sector will not be different from the regular case.

Rather more complicated is the situation where the extraordinary point lies within the support of the vertex we are considering but is not the vertex itself.

We now have to carry out subdivision down to the point where the extraordinary point is an explicit vertex influenced by the initial mask. Once we reach this point, we can express the support of the original vertex as being the union of the supports of the vertices at this level, and again we see that the nature of the overall support will be the same as in the regular case.

We thus come to the conclusion that the presence of irregularity in the form of extraordinary points in the polyhedron does not alter the nature of the support boundary, provided that each sector of the footprint of the extraordinary point is the same as that for a regular point.

7.2 Skew schemes

In [1] and [6] there is a classification of subdivision schemes which includes skew schemes. In these schemes the self similarity is expressed not only by a scaling of the footprint but with a rotation

as well. That is, in each step each already constructed point is substituted with a *rotated* image of the footprint. In fact, the $\sqrt{3}$ -scheme is an example of a skew scheme but we were able to study it as a non-skew scheme by taking double steps. That was possible because the rotational symmetry of the scheme, which is $\frac{\pi}{3}$, is an integer multiple of the rotation of the footprint, which is $\frac{\pi}{6}$. In general skew schemes, where the rotational symmetry of the scheme is not an integer multiple of the rotation of the footprint, we have to work with the generalized form of (9):

$$\mathbf{S} = \left\{ \sum_{m=1}^{\infty} \frac{e^{(m-1)(i\pi/\theta)}(n-1)}{n^m} P'_{i_m} \mid i_m = 0, 1, \dots, k \right\} \quad (35)$$

The term $e^{i\pi/\theta}$ represents the rotation of the footprint by an angle θ and the points of \mathbb{R}^2 can now be thought as a vector space over the complex numbers \mathbb{C} , or, even better, as complex numbers themselves. In this case (35) is a complex power series.

Another way to handle skew schemes is to alternate rotation direction on alternate steps. This allows us to consider double steps without rotation. An interesting feature of such alternating skew schemes is that they can have polygonal support without any pair of edges being parallel.

7.3 Higher dimensions

In the d -dimensional case the results on the $d-1$ dimension become results on the boundary and similar proof techniques are expected to apply. The main equation becomes

$$\mathbf{S} = \left\{ \sum_{m=1}^{\infty} \frac{(n-1)}{n^m} T^{m-1} P'_{i_m} \mid i_m = 0, 1, \dots, k \right\} \quad (36)$$

where T is an isometry of \mathbb{R}^d fixing the origin.

8 Discussion: support, artifacts and structure

The nature of the support influences the operational performance of a scheme through the question of lateral artifacts. It is well known that, if an attempt is made to run a feature skew to the isoparametric lines in a tensor-product patch system, it will be reproduced unevenly. To get a nice extruded feature it has to be run in one of the two isoparametric directions. Three-direction box-spline based schemes, such as Loop [9], have three directions in which features may safely be run, and the four-direction box-splines such as ‘simplest’ [10] and ‘4–8’ [11] have four.

For a direction to be safe, it is a necessary condition that the support should have a parallel pair of long enough⁴ straight boundaries in that direction. If a scheme has a totally fractal boundary there will be no directions in which features can be extruded exactly. We have examples of schemes (1) which are polygonal with pairs of parallel edges (e.g. Figure 3), (2) which have polygonal support without any parallelism between ‘opposite’ sides (e.g. some alternating skew schemes), (3) which are totally fractal (e.g. Figure 4(a)) and (4) which are fractal in parts of the boundary and straight in others (e.g. Figure 4(b)).

The support may also be a convenient way of establishing results about the structure of the limit surface. The best known schemes have a piecewise polynomial structure in regular regions, with nested rings of such pieces around extraordinary vertices. If a scheme has a fractal support boundary, it can at best have pieces meeting at fractal boundaries, and we speculate that it cannot have polynomial pieces at all.

9 Summary

We have studied the support of subdivision in terms of the arity and the non-zero values of the basis function after the first iteration of the scheme. In the cases where we were not able to calculate the

⁴Clearly, such boundaries will need to have a length at least equal to the distance between old vertices in the mesh.

support explicitly we studied its convex hull, the boundary of the convex hull and its interior, finding polygonal outer and inner bounds for the support. Our results provide useful insights into the behaviour of subdivision schemes.

Acknowledgements

This work has been supported by the European Union, under the ægis of the MINGLE project (HPRN-CT-1999-00117).

References

- [1] M. Alexa. Refinement operators for triangle meshes. *Computer Aided Geometric Design*, 19(3):169–172, 2002.
- [2] E. Catmull and J. Clark. Recursively generated B-spline surfaces on arbitrary topological meshes. *Computer Aided Design*, 10:350–355, 1978.
- [3] G. Deslauriers and S. Dubuc. Symmetric Iterative Interpolation Processes. *Constr. Approx.*, 5:49–68, 1989.
- [4] N. A. Dodgson, M. A. Sabin, L. Barthe, and M. F. Hassan. Towards a ternary interpolating subdivision scheme for the triangular mesh. University of Cambridge Computer Laboratory Technical Report No. 539, 2002.
- [5] D. Doo and M. Sabin. Behaviour of recursive division surfaces near extraordinary points. *Computer-Aided Design*, 10:356–360, 1978.
- [6] I. P. Ivriissimitzis, N. A. Dodgson, and M. A. Sabin. A generative classification of subdivision schemes with lattice transformations. University of Cambridge Computer Laboratory Technical Report No. 542, 2002.
- [7] V. Kannan. Cantor set: From classical to modern. *Math. Stud.*, 63(1-4):243–257, 1994.
- [8] L. Kobbelt. $\sqrt{3}$ -Subdivision. In *SIGGRAPH 2000 Conference Proceedings*, pages 103–112, New York, 2000. ACM.
- [9] C. T. Loop. Smooth subdivision surfaces based on triangles. Master’s thesis, University of Utah, Department of Mathematics, 1987.
- [10] J. Peters and U. Reif. The simplest subdivision scheme for smoothing polyhedra. *ACM Transactions on Graphics*, 16(4):420–431, 1997.
- [11] L. Velho and D. Zorin. 4–8 subdivision. *Computer Aided Geometric Design*, 18:397–427, 2001.
- [12] J. Warren and H. Weimer. *Subdivision Methods for Geometric Design*. Morgan Kaufmann, San Francisco, 2002.

Appendix

For an alternative arithmetic description of the ternary Cantor set we write the numbers of the interval $(0,1)$ in the triadic arithmetic system

$$x = .d_1d_2d_3\dots \quad d_i \in \{0, 1, 2\} \quad i = 1, 2, 3, \dots \quad (37)$$

The first step, that is, the removal of the middle third interval $(\frac{1}{3}, \frac{2}{3})$ will erase the numbers with $d_1 = 1$. The second step, that is the removal of the intervals $(\frac{1}{9}, \frac{2}{9})$ and $(\frac{7}{9}, \frac{8}{9})$ will erase the numbers

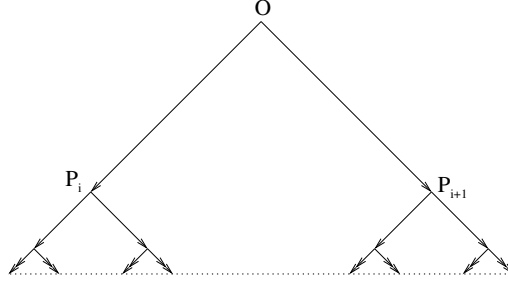


Figure 15: A description of Cantor's ternary set with the use of vectors.

with $d_2 = 1$ that were not erased in the first step. Continuing this way we remove all the numbers that have any 1 in their triadic expansion. Thus the ternary Cantor set can be thought of as the set of numbers in the interval $(0,1)$ with only 0s and 2s in their triadic expansion. This alternative description of the Cantor set was used in a part of the proof of Proposition 4.1.

For a third description of the Cantor set, we start with two linearly independent vectors $O\vec{P}_i$ and $O\vec{P}_{i+1}$ and create the sets

$$\left\{ \frac{1}{3^i} O\vec{P}_i, \frac{1}{3^i} O\vec{P}_{i+1} \right\} \quad i = 0, 1, \dots \quad (38)$$

Then we choose one element from each one of these sets and add them up. We notice that because

$$1 + \frac{1}{3} + \frac{1}{3^2} + \dots = \frac{3}{2}$$

all the points we can generate this way have the form

$$\lambda_1 O\vec{P}_i + \lambda_2 O\vec{P}_{i+1}, \quad 0 \leq \lambda_1, \lambda_2, \quad \lambda_1 + \lambda_2 = \frac{3}{2} \quad (39)$$

that is, they are points of the segment $P'_i P'_{i+1}$ defined by the endpoints of $\frac{3}{2} O\vec{P}_i$ and $\frac{3}{2} O\vec{P}_{i+1}$.

Nevertheless, not all the points of $P'_i P'_{i+1}$ are generated this way. For example, if we choose the vector $O\vec{P}_i$ from the first set then we have $\lambda_1 \geq 1$ while if we choose $O\vec{P}_{i+1}$ we will have $\lambda_1 \leq \frac{1}{2}$. Thus, in any case we cannot generate the points with $\frac{1}{2} < \lambda_1 < 1$, which are the points of the middle third interval of $P'_i P'_{i+1}$. Generally, the choice from the first k sets determines an interval of length $\frac{1}{3^k}$ in which the final point lies, while the choice from the next set determines if the final point lies in the right third or in the left third of that interval. It is not difficult to see that the subset of points of $P'_i P'_{i+1}$ we can reach in this process is the ternary Cantor set defined on $P'_i P'_{i+1}$ (Figure 15). This third description of the ternary Cantor can be used as an intuitive illustration of the way the boundary of a bivariate ternary scheme is constructed.